

Scintillation Scanning with an Eight-Inch Diameter Sodium Iodide (Tl) Crystal^{1,2,3,4}

J. G. McAfee,⁵ J. M. Mozley,⁵ T. K. Natarajan, G. F. Fueger, and H. N. Wagner, Jr.

Syracuse, New York

Since its introduction in 1951 by Cassen *et al* (10), rectilinear scintillation scanning has undergone progressive technical improvement. Among the most significant advances have been:

- (1) the multichannel focusing collimator, originated by Newell *et al* (29) and developed by Harris, Bell and Francis (15).
- (2) the use of pulse height analysis by Harris, Francis and Bell.
- (3) the display of the scanning image on photographic film by a light source initiated by Anger (1), and high contrast photorecording by Kuhl *et al* (20b) Bender and Blau (7) and Herring (17).
- (4) the use of three-inch diameter sodium iodide crystals by Bender and Blau (7) and Shy (29).

After 1958, the rectilinear scanner, with a three-inch diameter crystal and focusing collimator, has become a widely employed instrument for the delineation of the distribution of gamma-emitting radionuclides within various body organs. Two major limitations of this technique remain—firstly, the excessive time consumed for the completion of each scanning procedure and secondly, limitation

¹This work was supported by Research Program Project Grant #GM-10548 of the National Institutes of General Medical Sciences, U. S. Public Health Service.

²Presented at the 7th Annual Meeting of the Society of Nuclear Medicine, Berkeley, California, June, 1964.

³Technical assistance: Hallan, J. B., Ober, D. T. and Langan, J. K.

⁴Departments of Radiology and Radiological Science, The Johns Hopkins Medical Institutions, Baltimore, Maryland.

⁵Present address: State University of New York, Upstate Medical Center, Syracuse, New York.

of resolution to structures one-half to one-inch in diameter or greater. There appear to be six major factors that influence the resolution of the image of a scintillation scan—(1) the “optical” or geometrical configuration of each of the channels of the multichannel collimator; (2) the statistical variations in counting rate; (3) the fractional contribution of scattered photons to the total photon flux recorded by the detector; (this scattering may originate from the patient, the side-shielding or collimator septa); (4) septal penetration of photons with little or no attenuation; (5) photorecorder response time—the use of integrating or RC circuits for the contrast enhancement of photorecorded scanning images gives rise to “scalloping” of the margins of the organ images, resulting in a loss of resolution of both external contours and internal irregularities; (6) motion of the patient’s body during the scanning procedure, which becomes a major problem with long scanning times and restricts the use of this technique in severely ill and restless patients, and young children.

In practice, using three-inch diameter crystal detectors, the resolution is limited more by the relatively large statistical variations in counting rate than by the optical resolution of the collimator. To overcome this limitation, a scanning system was assembled with an eight-inch diameter crystal, to obtain higher counting rates and shorter scanning times. The use of a five-inch diameter crystal for this purpose was reported previously by Johns and Cederlund (18).

OVERALL DESIGN OF THE EIGHT-INCH CRYSTAL SCANNER

The detector is mounted in a steel frame¹ (overall dimensions 94 inches x 41 inches x 35 inches high) below a tabletop supporting the patient (Fig. 1A). The lead shield surrounding the detector is a uniform hollow cylinder with a wall thickness of three inches, an internal diameter of 9.75 inches and an external diameter of 16 inches. This 2,700 pound shield is supported on two parallel I-beams with heavy duty stainless steel bearings (Fig. 1B) which permit uniform transverse linear scanning speeds of 6-to-96 inches per minute with a minimum of vibration and noise. Although this scanning mechanism is heavy, it is mechanically much simpler than the conventional overhanging detector which scans the patient from above. The longitudinal spacing between adjacent scan lines may be varied from 1/16-to-1/4 inch in 1/16-inch increments. The maximum scanning area permitted by this instrument is 38 × 16 inches. An end-loading Bucky mechanism has also been mounted beneath the tabletop to permit routine radiographs of the body region being scanned without moving the patient.

Initially, plywood was used as the tabletop. However, this was completely unsatisfactory because of excessive absorption of weak gamma photons of 150 keV or less. A sheet of fiberglass reinforced plastic, one-eighth inch thick, was found completely satisfactory as a tabletop and was capable of supporting patients weighing up to 300 pounds.

A small hoist, mounted on one corner of the scanning frame, is used to change the heavy collimators which have an overall diameter of 9.75 inches and each of which vary from 60-to-85 pounds.

¹Ohio-Nuclear, Inc., Cleveland, Ohio.

With the detector mounted underneath the table, a mechanical interconnection between the moving detector and plotter is not convenient. The scanning images are recorded on a remote X-Y plotter whose recording head is driven in synchronism with the detectors by means of synchros. The recording head has a solenoid-driven stylus which produces an immediately visible display of the scanning image on 3M "Action" pressure-sensitive paper underlaid with this opaque black polyethylene sheeting, and a focused light source for photorecording. The plotter is enclosed in a light-tight box, and conventional 14×17 inches radiographic film in special cassettes is used for photorecording. The size of the recorded image is restricted by the cassette to a 13×16 inch area, but this is sufficient for almost all organs of the body even when pathologically enlarged. In the rare instances when it is necessary to scan areas larger than 13 inches, the full scanning area of 38×16 inches can be utilized by returning the X-Y plotter to the starting position and inserting an additional film.

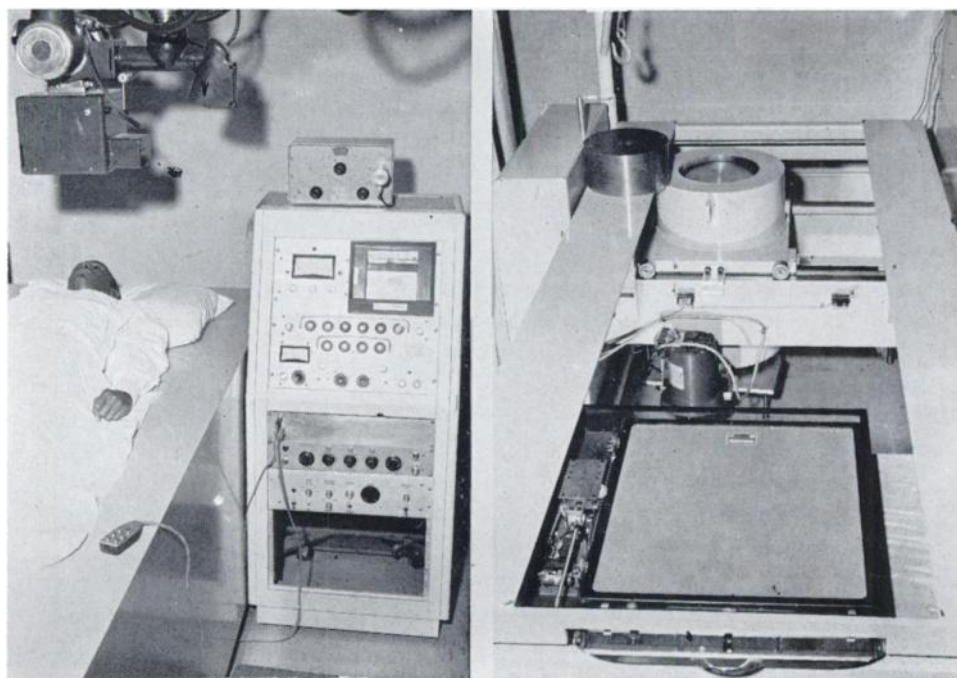


Fig. 1. Eight-inch crystal scanner.

(A) *Left:* Patient lying in supine position for pulmonary, renal or splenic scanning. Note the push-button controls for scanning motion placed on the tabletop, and overhead x-ray tube for superimposition radiographs. (B) *Right:* With tabletop removed the large cylindrical lead shield is seen surrounding the crystal and supported on two large I-bears. Note collimator on supporting ledge, hoist for lifting collimators, and Bucky mechanism in foreground.

DESIGN AND PERFORMANCE OF CRYSTAL ASSEMBLY

The eight-inch diameter crystal¹ with an overall thickness of four inches consists of an 8 × 2 inches thick thallium-activated sodium iodide crystal matched to an 8 × 2 inches thick pure sodium iodide crystal mounted in a low mass aluminum container. It is optically coupled to three RCA #8054 photomultiplier tubes with a low background "base assembly", and antimagnetic shields. The distal end of the activated crystal has a 45 degree bevel, one-half inch in width; therefore, the distal crystal surface adjacent to the collimator has a diameter of seven inches. This assembly is mounted in a chassis with a motor drive which permits the crystal to be raised and lowered within the cylindrical lead shield for use with collimators of varying thickness. The unactivated sodium iodide crystal serves as a light pipe for better light collection by the photomultiplier tubes and better pulse height resolution, and also serves to reduce the crystal background.

Although it was anticipated that the background counting rates of the eight-inch diameter crystal would be high, the attenuation afforded by the side shield, collimator and sodium iodide light pipe reduced these to tolerable levels. (Table I).

The background gamma-ray spectrum of the eight-inch diameter crystal within the lead shield showed an x-ray peak at 70 to 72 keV. This peak was undesirable, since it was in the same energy range as the important radionuclide mercury-197. This x-ray peak was presumably due to fluorescent radiation from

TABLE I

COMPARISON OF SENSITIVITY MEASURED WITH FLAT DISC REFERENCE SOURCES¹,
AND BACKGROUND COUNTING RATES FOR 3", 5" AND 8" CRYSTALS.
COLLIMATORS WITH IDENTICAL RADIUS OF RESOLUTIONS (R = .5")
DATA IN COUNTS PER MINUTE

Window (KEV) Base level setting (KEV) Source	80		80	
	84 ⁵⁷ Co	BKG	324 Mock Iodine	BKG
3" crystal scanner 19 hole collimator	16,000	160	11,500	100
5" crystal scanner 61 hole collimator	42,800	52	63,100	25
8" crystal scanner 119 hole collimator	104,000	270	119,110	75

¹Six-inch diameter flat disc reference sources prepared by New England Nuclear Corporation, were placed in contact with distal collimator face.

¹Harshaw Chemical Company, Crystal Division, Assembly Type 32MB8/AX

the scattering of high energy ^{40}K and cosmic photons in the lead shield. This x-ray peak was completely suppressed by a lining of 0.03 inches of cadmium foil within the lead shield, and an inner lining of 0.005 to 0.015 inches of copper foil immediately surrounding the sides of the crystal housing, as recommended by Heath (16).

The pulse-height resolution for a point source of cesium-137 eight inches from the crystal surface was 10 per cent, using a 10 keV window compared with resolutions of 7.5-to-9 per cent with three-inch diameter crystals, and 7.7-to-9.5 per cent for five-inch diameter crystals under the same conditions. There was no measurable shift in the base level of the cesium photopeak when measured through an outside hole of the collimator, compared with the central hole. Non-uniformity of pulse-height response in different regions of the detector was observed previously (18), with a five-inch diameter crystal two inches in thickness without an inactive sodium iodide light pipe, but did not occur with the eight-inch crystal assembly. The pulse-height resolution for weaker energy gammas was considerably poorer than for cesium-137. For example, for the 77 keV gamma and the 69 keV x-ray of ^{197}Hg the pulse height resolution was as poor as 18-to-20 per cent.

The improvement in counting rates for extended planar or volumetric sources of radioactivity can be estimated for crystals of different diameters approximately from the ratios of the areas of the distal crystal face. The nominal three-inch diameter crystal ordinarily has an actual diameter of 2.75 inches, and because of the bevel of the crystal rim, the five- and eight-inch diameter crystals have a true diameter of four and five-eighths inches and seven inches respectively at the crystal face (Fig. 2). By actual experiment with various sources and different collimators, the five-inch diameter crystal had an increased sensitivity over a three-inch crystal by a factor of three, and the eight-inch crystal by a factor of six-to-eight, using collimators with comparable radii of resolution. Specific examples of the relative counting rates are given in Table I.

From previous experience with lead and tungsten collimators for three-inch diameter crystals, the resolution for gamma photons in organ scanning approximately above 500 keV has been extremely poor. The crystal and collimator configurations of the eight-inch scanner were designed for the energy range of 25-to-500 keV. Hence, the activated portion of the crystal was limited to a thickness of two inches. From the Monte Carlo calculations of Miller (9, 25) the efficiency of an eight-inch diameter crystal two inches in thickness for a parallel beam of 279 keV gammas was 0.957, and the photofraction 0.919. On increasing the crystal thickness to four inches the efficiency at this energy is increased only four per cent and the photofraction only 2.5 per cent. In contrast, for a parallel beam source of 661 keV gammas of ^{137}Cs , the 8×2 inch crystal had an efficiency of only 0.749 and a photofraction of 0.631. The four-inch crystal thickness in this case increases the efficiency 34 per cent, and the photofraction 23 per cent.

¹Another crystal assembly of this type had a pulse height resolution for ^{137}Cs as low as 8.2 per cent.

ELECTRONIC COMPONENTS

The three photomultiplier output signals are summed ahead of the preamplifier. A preamplifier with a fixed gain of X 10 is housed beneath the crystal assembly within the lead shield. Separate high voltage and shielded signal cables are used between preamplifier and spectrometer. Extreme care must be exercised to eliminate ground loops. The spectrometer is a standard commercial-transistorized single-channel gamma spectrometer. A count rate meter is connected to the spectrometer for a preliminary assessment of the counting rates prior to the scanning procedure, but is not used in the generation of the scan image. With the high linear scanning speed used, integrating or rate meter circuits commonly employed in high contrast photoscanning with three-inch crystal detectors are unsatisfactory because of their slow response times. A photorecorder system was therefore designed and constructed with short response time to produce a varying degree of contrast enhancement of the photographic image, without displacement or scalloping of the scan image.

A block diagram of the recording system is given in Figure 3A. The photorecording system utilizes a Sylvania R1131C glow modulator tube. It is driven by a series transistor switch. Provision is made for modulating the glow intensity in accordance with the count rate. The transistor switch is triggered by pulses from the gamma-ray spectrometer. A scaler is supplied to reduce the pulse rate when desired.

The modulating signal is provided by a sliding pulse interval average technique. The pulses from the spectrometer are used to drive a 12-stage Dekatron tube (GS-12D) having suitable load resistors in the cathodes. As the glow switches from one cathode to the next, a capacitor is charged almost instantaneously and then allowed to discharge with a time constant of approximately two seconds. The discharge levels of all 12 such capacitors are summed to provide a rate signal which is used to modulate the glow tube at any instant when a pulse occurs. This rate signal is therefore proportional to the rate of occurrence of 12 consecutive pulses. A simplified schematic diagram of this rate signal generator is given in Figure 3B.

Background subtraction determined by the count rate is also provided as an optional feature in the system. The subtraction is purposely made a nonlinear function of the count rate. At count rate values at which subtraction is desired, (*i.e.* count rate values below a preselected level) the pulses driving the glow modulator tube are scaled down by factors increasing with decreasing count rate. The maximum scale factor of approximately 25, occurs at 75 per cent of the selected count rate level. Below the 75 per cent level, the pulses are prevented from triggering the glow modulator tube. Above this selected count rate level, the scale factor remains constant at two.

COLLIMATOR DESIGN

The most difficult problem in the construction of the eight-inch crystal scanner was collimator design. A number of workers previously studied in detail

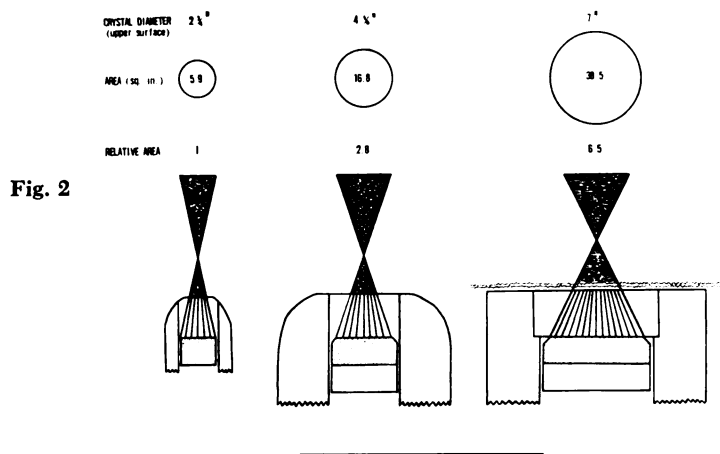


Fig. 2

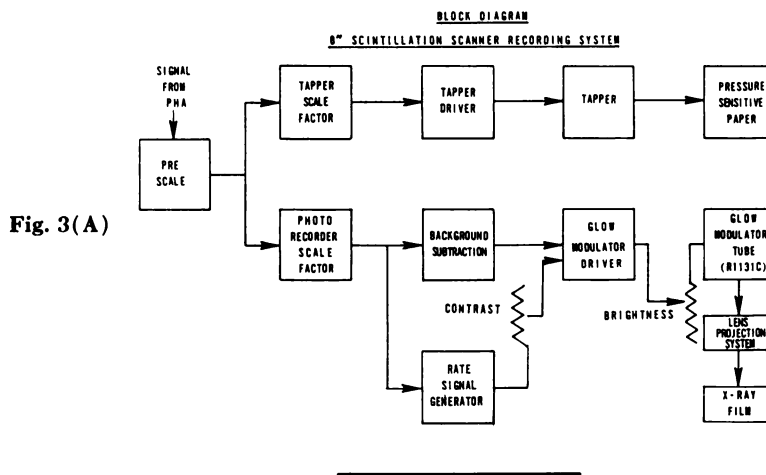


Fig. 3(A)

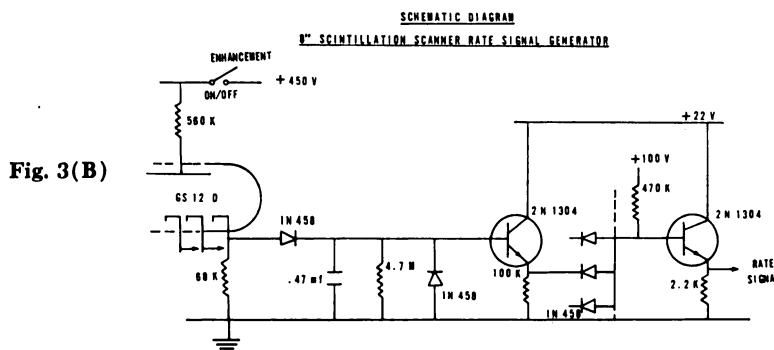


Fig. 3(B)

Fig. 2. *Top*: Comparison of geometry of normal three-inch, five-inch and eight-inch crystal scanners. The efficiency can be predicted approximately from the ratios of the surface areas of the lower crystal face. The five- and eight-inch diameter crystals are beveled. Because of the fiberglass tabletop, the focal distance for the eight-inch crystal is 3.5 inches, rather than three inches for the three- and five-inch crystals.

Fig. 3. (A) *Middle*: Block diagram of the recording system. (B) *Bottom*: Simplified schematic diagram of the "rate signal" generator. Rate signal is proportional to the rate of occurrence of 12 consecutive pulses, and is used to modulate the glow tube.

collimator geometry and the contribution of scattered radiation (3, 5, 15, 20A, 27, 28, 31, 32). Because the possible variations in the number, size, and configuration of the collimator channels were so great, and because the engineering costs were prohibitively high for collimators designed on an empirical basis, the collimators were designed using the theoretical concepts of Beck (3, 4, 5) and later tested for their validity.

Preliminary collimators with varying focal depths (f) up to five inches were tested. Although their depth response was better than with three-inch focal depths, there was considerable degradation of resolution close to the surface, accompanied by significant loss of sensitivity. All of the "optimal design" collimators studied subsequently had an arbitrary focal depth of 3.5 inches. About 0.25 inches of this depth is occupied by the fiberglass-plastic tabletop and underlying air space, so that the effective focal plane lies 3.25 inches above the tabletop. To reduce collimator costs, the 10% increase in sensitivity of hexagonal channels over round channels was sacrificed, and round holes in hexagonal array were used exclusively.

A program on the institutional IBM 1401 and 7094 computers was used to optimize several parameters. The focal depth, f , was arbitrarily varied from three-to-five inches in half-inch increments. The optical radius of resolution, R , was varied from one-sixteenth inch to one-inch (Fig. 4). The values of R of 1/4,

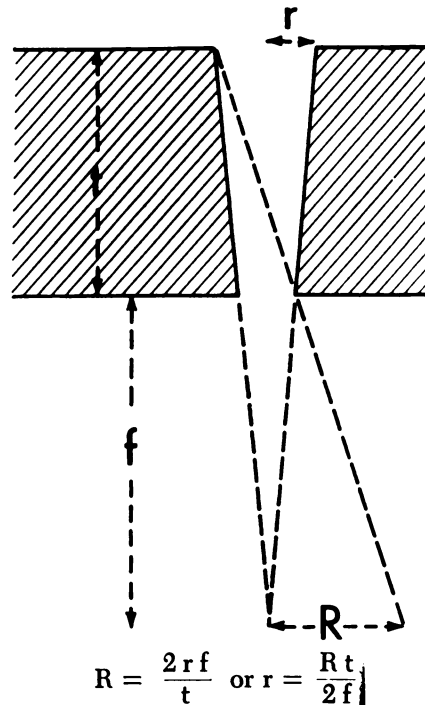


Fig. 4. Geometry of a single tapered channel. Collimator resolution, as determined by the optical radius of resolution R becomes worse as the radius r of the channel of the proximal collimator surface and the focal depth f increase. Resolution improves as the collimator thickness t increases.

3/8, and 1/2 inch were found to be practical for all gamma energies; a minimum value of one-eighth inch (maximal resolution) also appeared practical for energies less than 150 keV.

For collimator holes in hexagonal array, the total number of holes, N , is $3n^2 + 3n + 1$, where n is the number of concentric rings in the array. "n" was varied from one (seven-hole collimator) to 22 (1,519-hole collimator). In the surface of an eight-inch diameter crystal, there is considerable "unused" area outside the last complete ring of the hexagon, so that incomplete rings could be added to the array, thereby adding a number of additional holes at the periphery equal to $6n - 12$.

The radius of the holes at the "outlet" end of the collimator adjacent to the crystal was varied at 0.001-inch increments from a minimal value of 0.001 inches. Using all of the above values in varying combination, the theoretical efficiency, $E(\text{cm}^2)$, for uniform planar sources of radioactivity was computed for all possible collimator designs. The fraction (P) of the count rate due to gamma photons reaching the crystal by septal penetration was then computed using the linear attenuation coefficients in lead of various gamma energies.

In a computer study of 19, 37, and 61 hole collimators which have been used extensively for three-inch crystal detectors for scanning with ^{131}I , it was found that the penetration fraction P equalled approximately 0.05. In other words, in the empirically designed collimators of the past, a septal penetration of five per cent was tolerable, based on extensive subsequent clinical trial.

In the selection of the collimators for the eight-inch crystal, the design which produced, at a P fraction of 0.05, maximum efficiency E , was selected as the "optimum" design. The collimators so developed are depicted in Figure 5; the dimensions of their configurations are given in Table II.

Short-lived radionuclides with weak gamma emissions such as $^{99\text{m}}\text{Tc}$, ^{197}Hg , ^{133}Xe , ^{131}Cs , $^{103\text{m}}\text{Rh}$ are receiving great interest for radioisotopic imaging because they can be administered with safety in relatively large doses (24). "Optimally" designed collimators using Beck's original criteria (3) can not be constructed for these weaker emissions, particularly for large diameter crystals, because of engineering and cost limitations. The number of channels called for in these designs for five- and eight-inch diameter crystals is 1,500 or even greater and the minimal septal thicknesses required can not be fabricated. The collimator depths are relatively short, so that the maximum diameter of the hexagonally spaced hole array at the distal collimator face is relatively large. As a result, the resolution close to the collimator is poor. The criteria of collimator design for these weaker gamma emitters must therefore be different from those used for higher energies, and be governed by (1) a limitation in the number of channels, (2) the minimal obtainable septal thickness at the distal collimator face for the outermost ring of holes, (3) the collimator shape factor (Beck's factor k) which restricts the maximum diameter of the array at the distal collimator face. Considerations of the penetration fraction may be ignored at these lower energies. Collimators for these energies, although difficult to fabricate, have a predictable improvement in efficiency by a factor of two over the collimators optimal for the 364 keV gammas of iodine-131.

ANALYSIS OF RESPONSE OF COLLIMATORS FOR THE EIGHT-INCH CRYSTAL

Several experimental methods were employed in an attempt to assess the response of collimators for the eight-inch crystal and to compare it with the conventional three-inch crystal. The measurement of resolution by progressively decreasing distance between two point sources in air was found unsatisfactory because the results were so dependent on source strength and on variables in other components of the scanning system. Isoresponse measurements performed with point sources in air, as recommended by Harris (15) and others, are technically difficult to perform. Precise localization of the point source in relation to the collimator within a few thousandths of an inch is required to detect the differences between collimators with this method. We have preferred isoresponse measurements of point sources and volumetric sources one-half inch and one-inch in diameter, within a tissue equivalent scattering medium (Lucite or water), because these conditions more approximately close to those during actual scanning on patients.

Accordingly, 50 isoresponse measurements were performed using different collimators, sources, and gamma energies. A few representative curves are supplied in Figures 6 and 7. It proved difficult to draw conclusions about collimator performance by analysis of these curves. In general, the depth response of the eight-inch crystal collimators was superior to that of three-inch crystal collimators as indicated by the depth of the 100 percentile point. However, the 10 percentile curves tended to be somewhat wider: the 1.0 and 0.5 per cent curves tended to be narrower and to extend downwards to a shorter depth for the eight-inch crystal. The depth response of the eight-inch collimators tended to extend over a narrower range than for three-inch crystal collimators at the 50% response level, but the difference was not remarkable at the lower response levels.

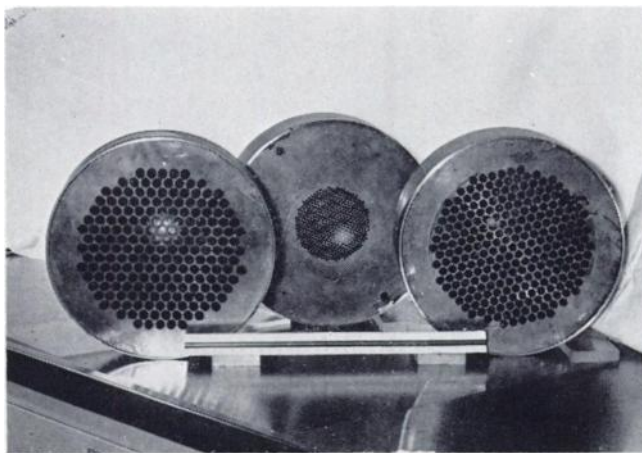


Fig. 5. *Top*: Lead collimators optimal for the 364 keV gamma photons of ^{131}I . Left to right—collimator E 199 holes, collimator C 439 holes (distal face) and collimator D 253 holes (Table I).

TABLE II
 "OPTIMAL" COLLIMATOR DESIGNS FOR 8" DIAMETER CRYSTAL
 (EFFECTIVE CRYSTAL DIAMETER 7"; FOCAL DEPTH $f = 3.5"$, PENETRATION FRACTION $P = .05$)

Radius of resolution R (inches)	No. of holes N	Taper half angle of holes (degrees)	Radius of holes proximal face (inches)	Minimal septal thickness proximal face (inches)	Minimal septal thickness distal face (inches)	Collimator depth t (inches)	Efficiency cm^2	Collimator Designation
.25	439 (397 + 42)	1.017	.122	364 KEV (^{131}I) .063	.023	3.42	1.16×10^{-2}	C
.375	253 (217 + 36)	1.483	.176	.0635	.033	3.29	3.03×10^{-2}	D
.5	199 (169 + 30)	1.750	.187	.099	.057	2.62	5.59×10^{-2}	E

.25	199 (169 + 30)	1.236	.191	510 KEV ($Sr^{85}Ga^{68}$) .089	.035	5.37	$.734 \times 10^{-2}$	H
.375	109 (91 + 18)	1.774	.258	.132	.056	4.82	1.87×10^{-2}	I
.5	73 (61 + 12)	2.251	.306	.184	.083	4.30	3.56×10^{-2}	J

In comparison of four different gamma energies, the best isoresponse curves for various collimators of different resolutions were obtained as a rule with ^{131}I (364 keV), but sometimes with ^{57}Co (123 keV). Iodine-131 produced "superior" curves to ^{57}Co for point sources and one-half inch spherical sources for most collimators, but ^{57}Co appeared better for one-inch spherical sources. For ^{197}Hg (69 and 77 keV) the maximum response usually occurred at a depth of 2.5 inches because of absorption of these weak photons within the phantom; furthermore,

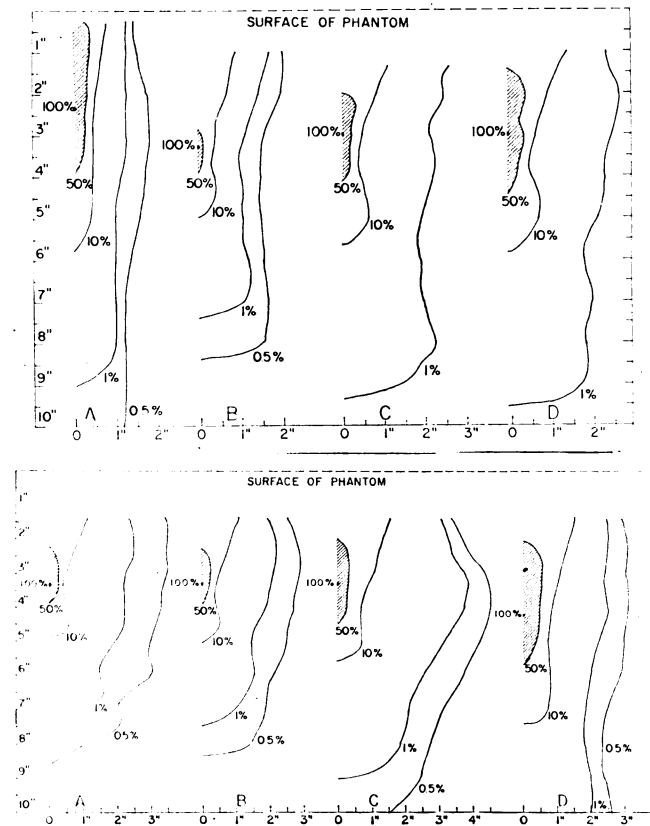


Fig. 6. Middle: Isoresponse curves in Lucite phantom, using ^{131}I . Base level setting 324 keV, window width 80 keV. Shaded area encloses 50 per cent contour.

(A) Three-inch crystal scanner with 37 hexagonal hole ORNL collimator, 0.5 inch diameter spherical source.

(B) Eight-inch crystal scanner with collimator C, 0.5 inch diameter spherical source.

(C) Same collimator, point source.

(D) Same collimator, one inch diameter spherical source.

Fig. 7. Bottom: Isoresponse curves of eight inch scanner using various radionuclides in 0.5 inch spherical source in Lucite phantom. Shaded area encloses 50 per cent contour.

(A) ^{197}Hg base level setting 64 keV window 30 keV collimator C

(B) ^{57}Co base level setting 98 keV window 50 keV collimator C

(C) ^{85}Sr base level setting 472 keV window 40 keV collimator C

(D) ^{85}Sr thicker collimator septa, but same settings as in (C).

For ^{131}I , see Figure 6 (B).

the 1.0 per cent and 0.5 per cent curves tended to be considerably wider than for ^{131}I , but the depth response slightly better. For all energies, whenever the radius of the spherical sources exceeded the radius of resolution of the collimators, their response appeared similar.

Collimators were evaluated also by measurement of the "Target/Non-Target ratio" of Bender and Blau (6, 7). The "non-target" count rates were measured in a Lucite tank 15 cm filled with radioactive solution. The "target" count rates were obtained with spherical sources of varying diameters filled with radioactive solution of the same concentration: the sphere was placed at different depths along the central axis of the collimator within the water-filled tank.

Some of these ratios are shown in Figures 8 and 9. Like the results of the isoresponse curves, the ratios indicate that the resolution close to the face of the collimator is poorer for the eight-inch diameter crystal than the three-inch crystal, for collimators of the same "optical radius of resolution." Nevertheless, at depths greater than 5 to 6 cms, the ratios for the eight-inch crystal are either equivalent to, or better than those of the three-inch size. For the same collimator and same size sphere, the highest ratios were obtained with iodine-131. The ratios for ^{57}Co were consistently higher than for ^{197}Hg , and those for ^{85}Sr were the lowest of the four nuclides studied. As would be expected, the ratios decrease rapidly for spheres of decreasing diameter. The ratios obviously change also as the size of the tank is altered.

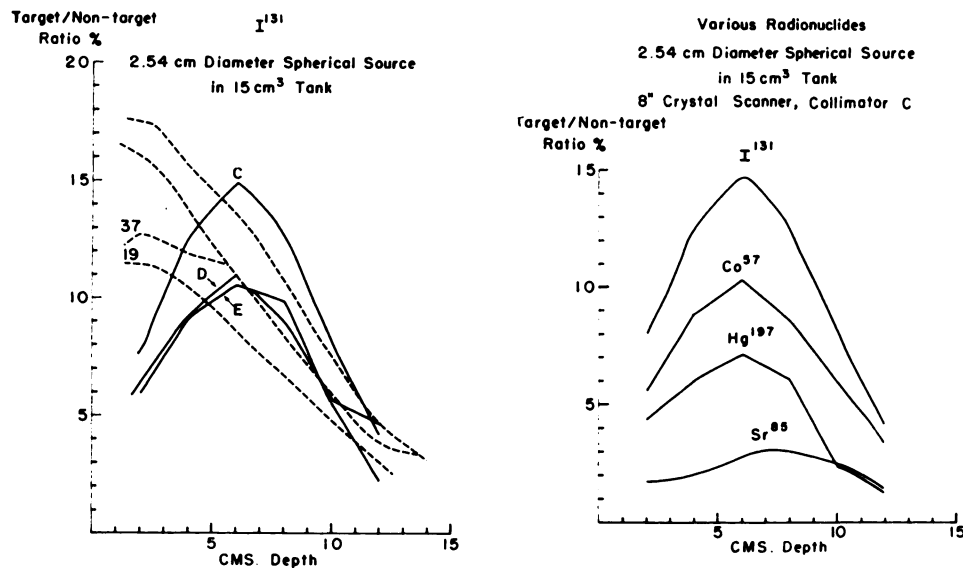


Fig. 8. Left: Target/Non-target ratios of Bender and Blau for ^{131}I . Dotted lines—31, 61, 37 and 19 hole collimators with three inch scanner. Solid lines—collimator C, D, and E with eight-inch scanner. Beyond a depth of 5 - 6 cm, ratios of three-inch and eight-inch scanners were similar. This was observed also for smaller spherical sources.

Fig. 9. Right: Target/Non-target ratios for various radionuclides. Ratios were observed best for ^{131}I , poorest for ^{85}Sr .

For both isoresponse curves and target/nontarget ratios, the results are heavily dependent on the settings of the spectrometer. For the weaker energy radio-nuclides in particular, they are markedly improved by using narrower window settings of 25 to 30 keV and an asymmetrical window, as recommended by Harris (13). In this situation, the base level setting appears even more critical than the window width. The settings used for the collimator measurements of this paper are not necessarily optimal for actual clinical scanning. By using narrow windows with "poor resolution" collimators, the results frequently can be made comparable to a "high resolution" collimator, at a sacrifice in sensitivity.

Isoresponse and target/nontarget measurements assess only resolution. Several figures of merit for comparison of different collimator-detector combination have been described in the literature (4, 12, 22), which attempt to consider the sensitivity in addition to the resolution. The values appear to be invariably superior for the eight-inch crystal detector, compared with the three-inch size, because of its greater efficiency.

More efficient and useful methods for characterizing the resolution of optical, photographic and x-ray imaging devices utilize the concept of the modulation transfer function (MTF). (26, 30). This function represents the relative amplitude response of a given imaging component or system to sinusoidal test objects of varying frequencies. In Figure 10, are presented the modulation transfer functions of the eight inch detector using collimators C, D, and E, whose detailed

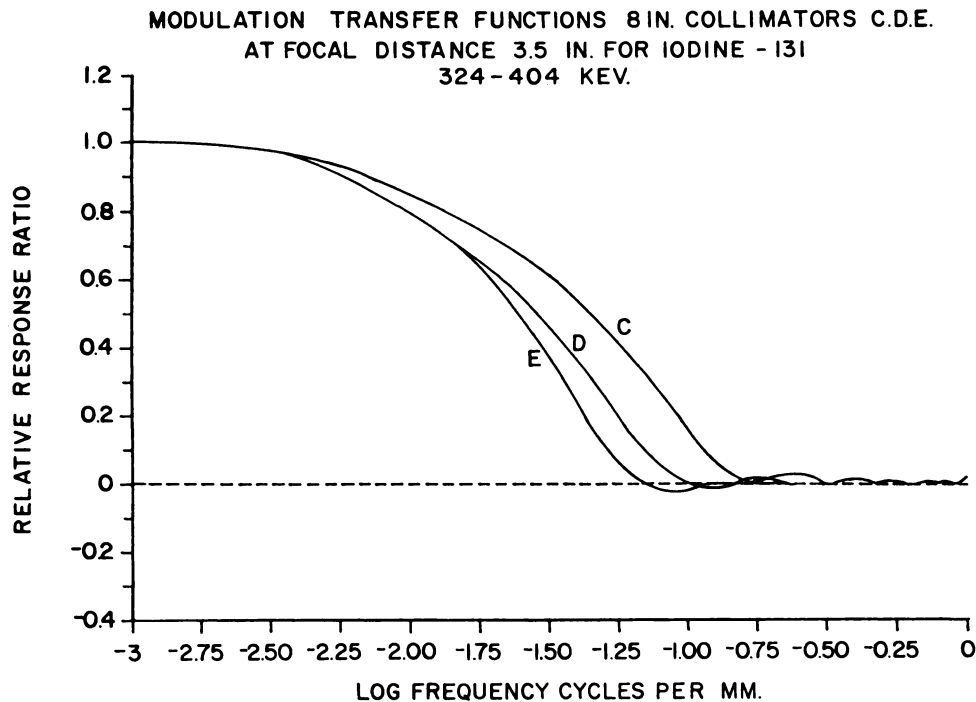


Fig. 10. Modulation transfer function curves for eight inch collimators C, D and E. Data for ^{131}I at geometrical focal distance of 3.5 inches.

specifications are listed in Table II. The modulation transfer functions in Figure 9 apply specifically to ^{131}I (324–404 keV) for objects lying on the focal plane (3.5 in). The modulation transfer functions were calculated from experimentally measured line spread functions by means of Fourier transformation. The curves in Figure 9 support clearly the observation in clinical use that not much difference in resolution can be seen between the D and E collimator, whereas collimator C has superior resolution.

PHANTOM STUDIES

Using the Picker thyroid phantom filled with 10 microcuries of ^{131}I solution, comparative scans were made on three-, five- and eight-inch crystal scanners, using linear scanning speeds of 6, 12 and 48 inches per minute respectively. The superiority of the larger crystal scanner is evident in Figure 11.

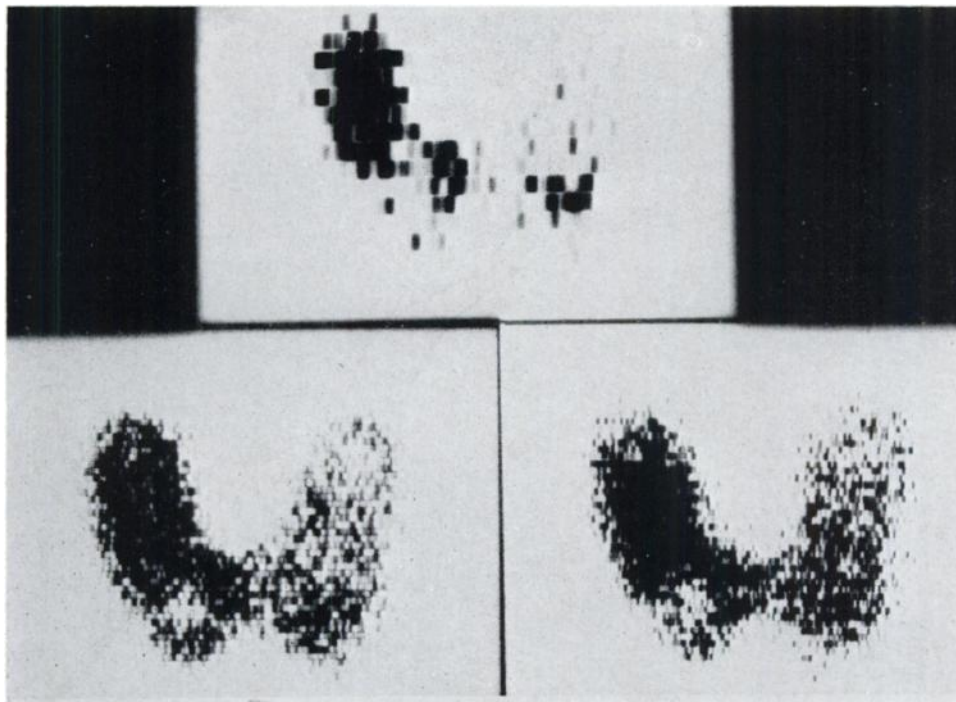


Fig. 11. Picker thyroid phantom filled with 10 μC ^{131}I .

12 mm diameter cylindrical defect right lower pole, 9 mm defect at left upper pole, 5 mm defect at right upper pole.

12 mm cylindrical cavity, left lower pole.

(A) 37 hole collimator with three inch scanner, linear speed six inches, per minute, line spacing $3/16$ in, area speed $1.125 \text{ in.}^2/\text{min}$.

(B) Eight-inch scanner, linear speed 48 inches per minute, line spacing $1/16$ in., area speed $3 \text{ in.}^2/\text{min}$.

(C) Five-inch scanner, linear speed 12 inches per minute, line spacing $1/16$ in., area speed $0.75 \text{ in.}^2/\text{min}$.

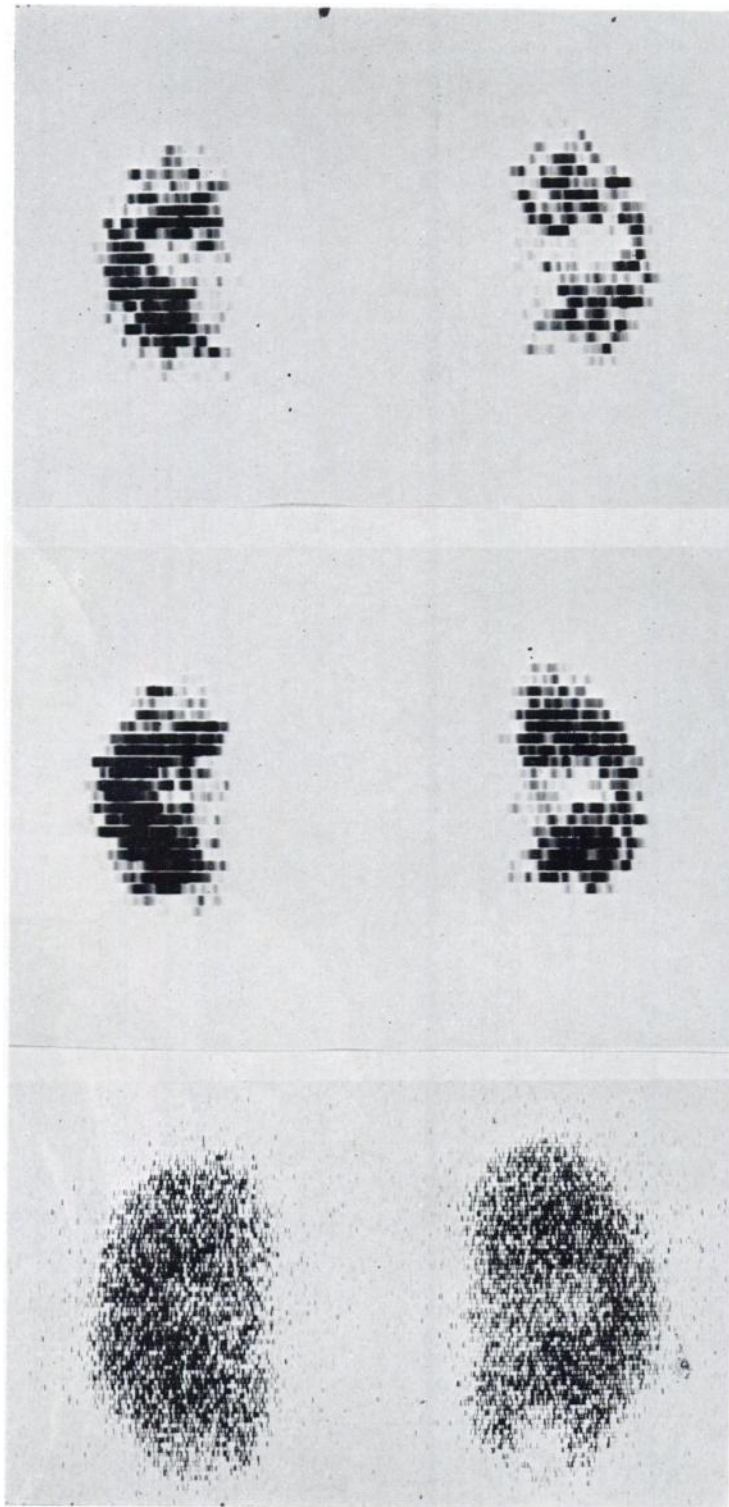




Fig. 12. Kidney phantoms each filled with $40 \mu\text{C } ^{203}\text{Hg}$, at a depth of 7 cms in Lucite. Left kidney—central and lower pole spherical defects one-inch in diameter. Right kidney—central and lower pole spherical defects $3/4$ -inch in diameter, $1/2$ -inch defect in right upper pole.

(A) *Opposite-Top*: 37 hole and (B) *Opposite-Middle*: 19 hole collimators with three-inch scanner, linear speed 12 inches per minute, line spacing $3/16$ in., area speed $2.25 \text{ in.}^2/\text{min}$, (C: *Opposite-Bottom*, D: *Top*, and E: *Bottom*) eight-inch scanner with collimators C, D and E respectively; linear speed 48 inches per minute, line spacing $1/16$ in., area speed $3 \text{ in.}^2/\text{min}$.

The collimators used for the three-inch and eight-inch scanners were optimum for ^{131}I as described above. The collimator for the five-inch scanner was not optimum for iodine-131. Therefore, a much smaller area speed was used for the five-inch scanner in these tests. Collimators for five-inch scanners, optimum for ^{131}I , are now available and should provide significantly improved performance.

A renal phantom was constructed out of Lucite, modeled from a pair of normal human kidneys removed at autopsy. The left kidney phantom contained two one-inch diameter spherical "tumors," one lateral to the renal hilus within the deepest portion of the kidney and the other at the periphery of the lower pole. Corresponding spheres three-fourths inch in diameter were placed in the right kidney and additional defects one-half inch in diameter placed in the right upper pole. These kidney-shaped phantoms were filled with 40 microcuries of either ^{197}Hg or ^{203}Hg and placed at various depths within the Lucite phantom (the plane of the kidneys was assumed to be an average of 2.75 inches deep from the surface). With both the three- and eight-inch crystal scanners, the defects could be demonstrated better with ^{203}Hg than with mercury-197. The results for the latter nuclide were markedly improved using an asymmetrical window setting of the pulse height analyzer of 65 to 90 keV, but nevertheless the resolution was still slightly inferior to mercury-203. Figure 12 reveals that the margins of the phantom kidneys, the defects of the renal hili, and the "tumor" defects were demonstrated better with the eight-inch scanner compared with the three-inch scanner, simply because of the improved counting statistics. With the eight-inch scanner the defects one-inch and 3/4-inch in diameter could be seen consistently; the 1/2-inch defect at the right upper pole was occasionally detected and the 1/2-inch defect in a thicker portion of the kidney was never demonstrated.

The area scan speeds, and thus the total scan times were roughly comparable for the two scanners: 2.25 in²/min for the three-inch unit and 3.0 in²/min for the eight-inch unit. The smaller line spacing used with the large crystal scanner contributes significantly to the improved resolution obtained.

CLINICAL RESULTS

Following the preliminary collimator resolution and phantom tests, the eight-inch crystal scanner was used first for human diagnostic studies in February, 1964. Since then, over 300 patient examinations have been completed. In many instances, the clinical results have been compared with corresponding scans performed with a conventional three-inch crystal detector. A few examples of clinical scans are shown in Figures 13 through 16 and other examples are illustrated elsewhere (23, 24, 34). All of the different types of organ scanning which could be carried out on the three-inch scanner could be obtained with an eight-inch scanner within a fraction of the time. For example, each projection of a brain scan (Fig. 13) could be completed in six-to-eight minutes at a linear speed of 96 inches per minute.

Flexibility in technique, including the choice of collimator, linear scanning speed and line spacing proved to be essential to fit the needs of different clinical applications. As a rule, high resolution scanning was used for the detection of

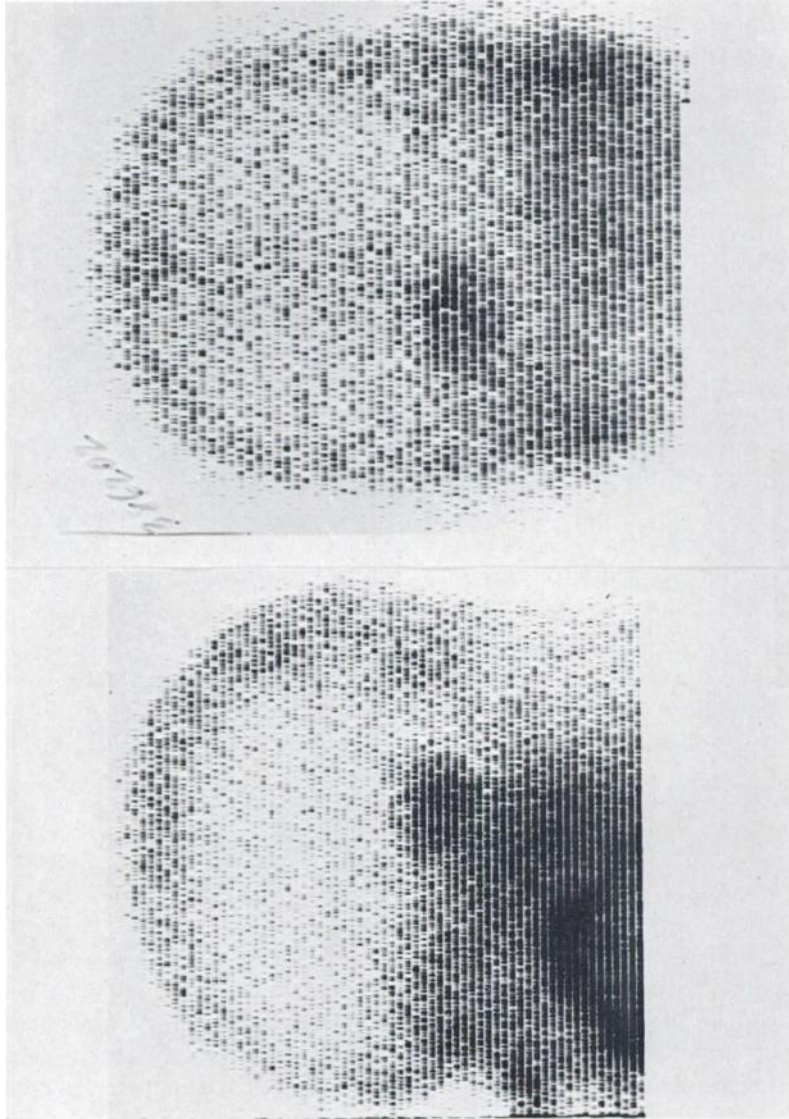


Fig. 13. (A) *Left*: Lateral and (B) *Right*: posterior projection brain scans, one hour after 10 mC. ^{99m}Tc pertechnetate IV. Cerebello-pontine angle metastatic tumor is easily seen. Collimator D; scanning speed 96 inches per minute.

small space-occupying lesions of the kidneys (Fig. 14). On the other hand, coarse resolution with a more efficient collimator, a line spacing of $1/8$ or $3/16$ of an inch and linear speed of 96 inches per minute was used in placental localization (23), in rapid pulmonary scanning searching for large defects in acute pulmonary vascular obstruction (34), and in studies in children (Fig. 15). In mediastinal scanning, the margins of the intravascular blood pool could frequently be defined more clearly with the eight-inch scanner because of the improvement of counting rates (Fig. 16).

The one outstanding disadvantage of the large eight-inch detector was encountered in hepatic scanning. The solid angle of the crystal-collimator assembly subtended at the focal point (45 to 60°) is larger than the three-inch detector (25°) or five inch detector (40°). In the geometry of liver scanning (Fig. 17A) the large detector "sees" a relatively large volume of tissue containing a high concentration of radioactivity close to the collimator face. As a result, small defects close to the surface are more difficult to demonstrate than with detectors with a smaller solid angle. On the other hand, in brain scanning (Fig. 17B) where only a thin layer of high radioactivity in the scalp and muscle is close to the detector, the increased solid angle has not been a problem. In renal scanning, where there is little or no radioactivity in the tissues superficial to the kidneys (Fig. 17C), the large solid angle has had no demonstrable adverse effect.

The location of the eight-inch detector beneath the tabletop is no hindrance for most types of organ scanning, compared with the conventional detectors suspended over the patient. The "under-the-table" location is superior in pulmonary, splenic and renal scanning where posterior projections may be obtained with the patient supine. Although thyroid and hepatic studies must be performed in the prone position, any patient discomfort is avoided by the short procedure times. For placental scanning (23) in the prone position during the last trimester of pregnancy, the patient can be comfortably positioned on thick foam rubber cushions under the chest and thighs.

When localization radiographs are obtained on the scanning table for superimposition of the photorecorded scanning image, the radiographic magnification is much less than in the conventional scanning position since the organ under study is adjacent to the tabletop and therefore closer to the x-ray film.

EIGHT-INCH CRYSTAL SCANNER VS SCINTILLATION CAMERAS

In exploring the potential of large detector high-speed scintillation scanners, one must consider the ever increasing possibility of development of a stationary scintillation camera which might perform the same imaging function. However, at the present state of development, scintillation cameras can not be considered as generally satisfactory alternatives to scanners.

The practical disadvantages of all types of cameras developed thus far are increased cost and limitation in field size to a maximum effective diameter of nine inches. Several large body organs already being scanned routinely such as the enlarged liver or spleen, both lungs, or the gravid uterus cannot be included in a single exposure with such a field size. On the other hand, serial pictures

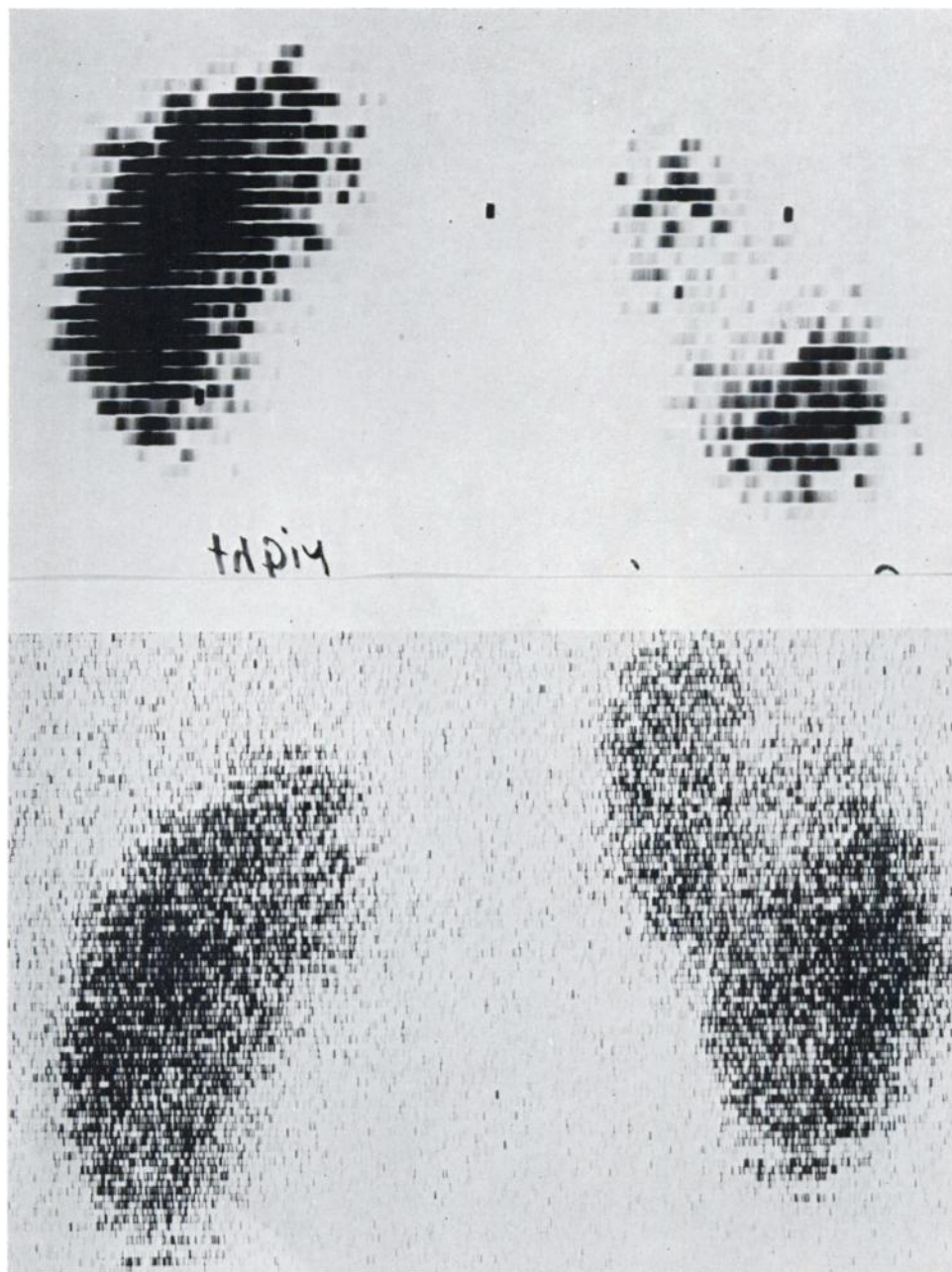


Fig. 14. Mercury-197 chlormerodrin renal scans. Hypernephroma of left upper kidney.

(A). *Top*: Three-inch scanner. The left kidney appeared slightly smaller than the right and the defect appeared large with the use of high contrast enhancement.

(B). *Bottom*: Eight-inch scanner. The kidneys appeared equal in size without the use of high contrast enhancement. The true size of the tumor was more accurately depicted as confirmed at surgery.

within intervals of a few seconds, which may be important in the future for dynamic function studies, are easily obtainable with cameras but are not possible by *conventional* scanning.

Cameras using a single slab of sodium iodide 11 inches in diameter x 1/2 inches thick with a bank of photomultiplier tubes possess resolution of the same order as conventional scanners (2, 11). Although the cameras have a reputation for higher sensitivity, comparisons of the past have been made with small crystal scanners. At higher energies, from 300 to 510 keV, the increased sensitivity compared with an eight-inch crystal scanner is slight. In cameras of the "pin-hole" type, the sensitivity falls off towards the edge of the large crystal (21). There is also a peripheral degradation in resolution beyond a radius of about three inches from the center (11). Variations in light photon collection from different locations within a large crystal contribute to the nonuniformity of response to point or line sources for stationary cameras, but not for moving detectors. Using the pin-hole geometry, the magnification factor is not linear throughout the entire crystal surface and varying degrees of shape distortion occur (21). This latter problem does not exist with camera collimators of the multiple parallel-hole type.

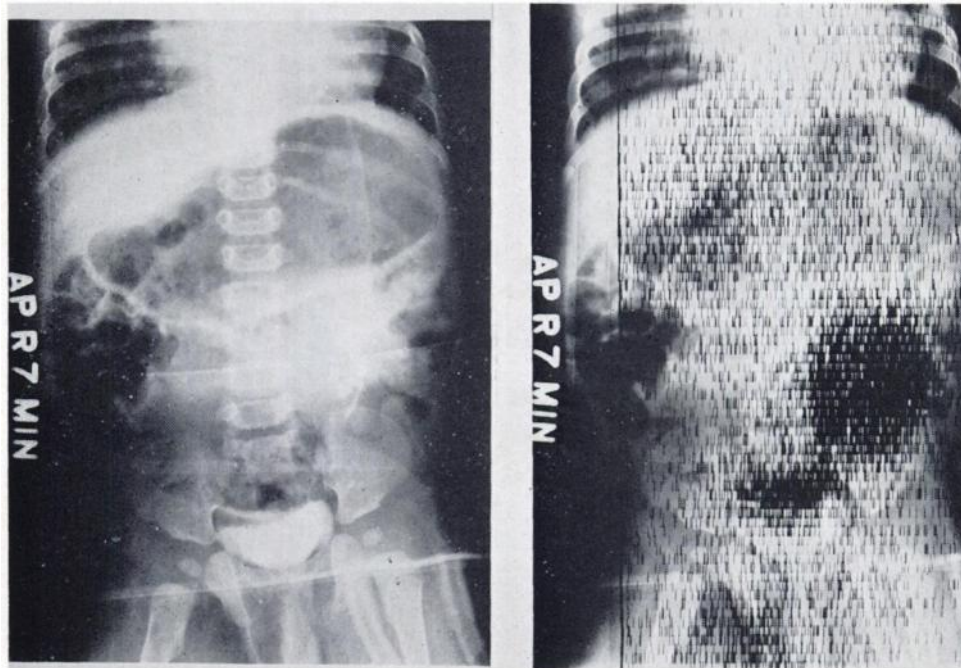


Fig. 15. Congenital unilateral "pancake" kidney in young child.

(A) *Left:* Intravenous urogram. A single renal collecting system with anomalous position of calyces and ureters seen in left lower abdomen.

(B) *Right:* Rapid "low resolution" scan after 30 uC Mercury-197 chlormerodrin at linear speed of 96" per minute and index spacing 3/16". Abnormally large area of functioning renal parenchyma is seen at the left lower abdomen and none on right. Note accumulation in the bladder.

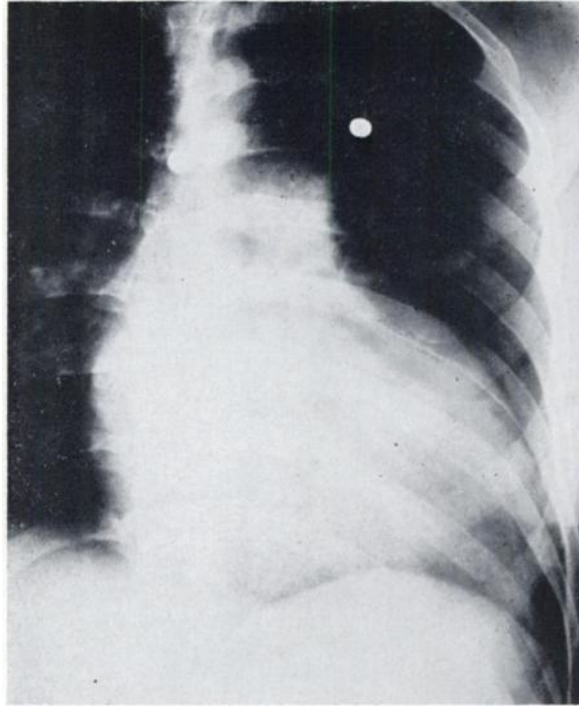
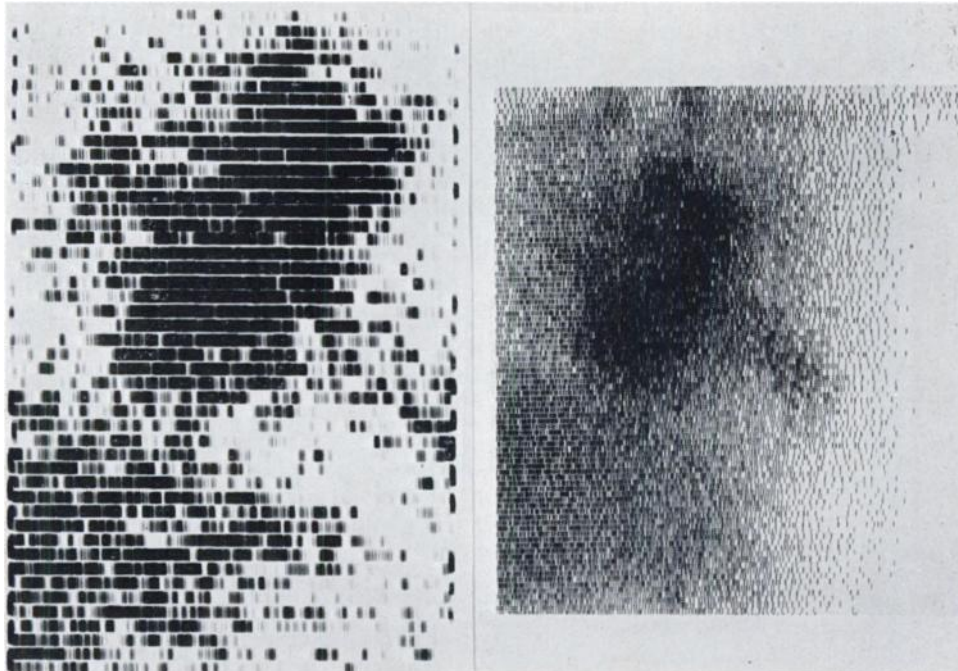


Fig. 16. (A). *Top*: Radiograph shows enlarged cardiac silhouette, dilated pulmonary artery. Question of pericardial effusion.



(B). *Left*: Mediastinal scan after 100 uCi. Iodine-131 albumin with three-inch crystal scanner at six inches per minute.

(C). *Right*: Mediastinal scan after one mCi. ^{99m}Tc albumin with eight-inch crystal scanner, at 96 inches per minute. No evidence of pericardial effusion. Dilated pulmonary artery segment. Avascular margin surrounding left ventricular chamber associated with marked myocardial hypertrophy is demonstrated.

These collimators are easier to fabricate than the focusing collimators of the large crystal moving detectors. With parallel-hole collimation, X-Y axis positional errors due to photon scattering within a crystal one-half inch in thickness are slight (21). However, the resolution degrades as the source-to-collimator distance is increased.

For all cameras using photomultiplier tubes, the major source of spatial error in resolution is due to the Gaussian spread in electron emission at each of the dynodes (11). As a result, point sources of radioactivity appear as disc sources of varying diameter, regardless of the fine resolution of the collimator system. This problem is worse at weaker gamma energies.

Cameras using a matrix of small sodium iodide crystal elements instead of a single large crystal, such as the autofluoroscope (7), have a greater sensitivity at higher gamma energies because of increased crystal thickness. The resolution thus far has been inferior to either conventional scanners or single-crystal cameras. There is considerable variation in response between one crystal element and another which becomes worse as the length-to-diameter ratio of each element increases. The spatial errors in resolution due to variations in photomultiplier tube response are the same as for the large single crystal camera. Spatial differences in radioactivity patterns can be readily quantitated by the autofluoroscope. Quantitation of a relatively static distribution of radioactivity within a region of the body is readily accomplished also by rectilinear scanning with a digital readout and storage system.

Stationary cameras using modified x-ray image intensifiers (33) and fine parallel-hole multichannel collimators have achieved a degree of resolution superior to any other system. They have an inherent advantage that the X-Y spatial information is accurately preserved from the site of photo-electron conversion throughout all of the stages of amplification. The lack of pulse-height selection,

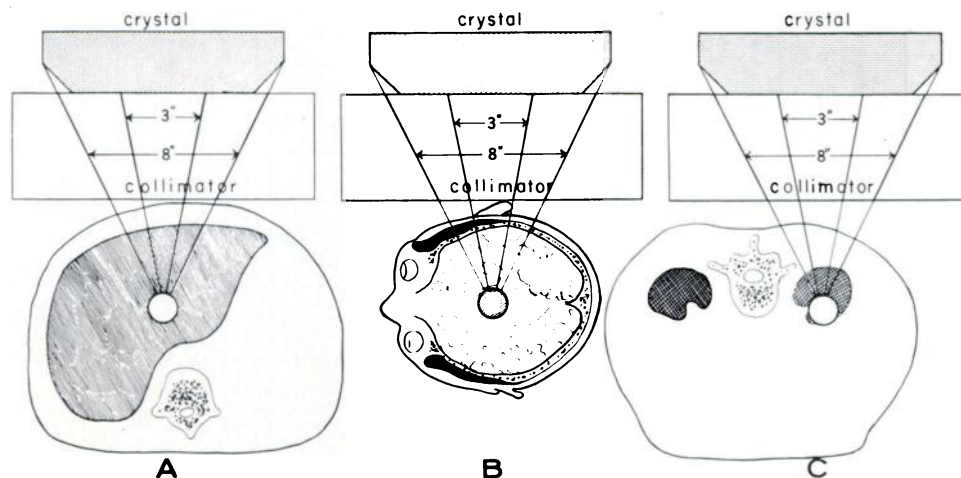


Fig. 17. Comparison of the effect of solid angle of three- and eight-inch scanners in organs with different geometrical configurations.

(A) Liver. (B) Brain. (C) Kidneys.

nonuniformity of response throughout the photo-emissive surface, and the poor efficiency of gamma-photon conversion above about 150 keV appear to be the chief limitations of this instrument.

Since each type of imaging system has its drawbacks, it is likely that both moving scanners and stationary cameras will be required in the future for different clinical applications. For static imaging, rectilinear scanners have proven versatility for a variety of field sizes and a relatively wide range of gamma energies.

CONCLUSIONS

The use of an eight-inch diameter sodium iodide crystal with focusing collimator for rectilinear scanning has been shown to improve the quality of scanning images and to shorten significantly the procedure times compared with a three-inch diameter crystal detector. The large crystal scanner has been superior for all types of organ scanning with the exception of the liver. Because of the greater number of patient studies which can be completed per day compared with a three-inch scanner, the increase in cost of the eight-inch scanner can be justified economically. The large crystal scanner is electronically less complex and less expensive than any type of scintillation camera.

So far, the collimators designed for this instrument have had the same optical resolution as those in common use for three-inch scanners ($R = 0.25$ to 0.5 inches). In the future, however, an improvement in the radius of resolution by a factor of two is theoretically feasible, particularly for radionuclides with weak gamma energies of 150 keV or less. The present limitation in the use of this instrument is imposed by engineering difficulties in the precise fabrication of focusing collimators for low gamma energies with extremely thin septa and a large number of channels. The maximum linear scanning speed of the unit described herein is 96 inches per minute; however, this should be increased to 400 inches per minute in the immediate future. Using such high scanning speeds, analog methods of photorecording are completely unsatisfactory. The need for high contrast photorecording, used extensively with three-inch scanners is considerably less with the larger crystal, because of the marked improvement in counting statistics.

For certain organs, such as the brain, liver and lungs, the optimal crystal geometry may consist of two opposing five-inch crystal detectors, rather than a single eight-inch crystal. Although the "double five-inch scanner" has an overall efficiency equivalent to a single eight-inch scanner, its cost is considerably greater because of the duplication in electronic components and image recording systems.

REFERENCES

1. ANGER, H. O.: A multiple scintillation counter in vivo scanner. *Am. J. Roent.* **70**:605-612, 1953.
2. ANGER, H. O.: Gamma-ray and positron scintillation camera. *Nucleonics* **21**:56-59, 1963.
3. BECK, R. N.: A theoretical evaluation of brain scanning systems. *J. Nuc. Med.* **2**:314-324, 1961.

4. BECK, R. N.: A theory of radioisotope scanning systems. *Medical Radioisotope Scanning*, Vol. I., Symp. Proc. IAEA, p. 35, Vienna, 1964.
5. BECK, R. N.: Collimators for radioisotope scanning systems. *Medical Radioisotope Scanning*. Vol. I., Symp. Proc. IAEA, p. 211, Vienna, 1964.
6. BENDER, M. A.: Photoscanning, pp. 31-40, *Medical Radioisotope Scanning*. Proceedings of IAEA & WHO, Vienna, February, 1959, published by the International Atomic Energy Agency, Kaertnerring II, Vienna.
7. BENDER, M. A. & BLAU, M.: A versatile high contrast photoscanner for the localization of human tumors with radioisotopes. *Inter. J. Appl. Rad. & Isotopes* 4:154-161, 1959.
8. BENDER, M. A. & BLAU, M.: The autofluoroscope. *Nucleonics* 21:52-56, 1963.
9. BIRKS, J. B.: The theory and practice of scintillation counting. Pergamon Press; The MacMillan Co., New York, 1964. Chapter 12. Alkali halide crystal scintillations and their applications. pp. 470-508.
10. CASSEN, B., CURTIS, L., REED, C. & LIBBY, R.: Instrumentation for I-131 use in medical studies. *Nucleonics* 9:46-50, 1951.
11. CRADDUCK, T. D. FEDORUK, S. O.: An experimental determination of the overall spatial resolution of a scintillation camera. *Phys. in Med. & Biol.* 10:67-76, 1965.
12. DEWEY, W. C. & SINCLAIR, W. K.: Criteria for evaluating collimators used in In Vivo distribution studies with radioisotopes. *Int. J. Appl. Rad. & Isotopes* 10:1-16, 1961.
13. HARRIS, C.: Certain fundamental physical considerations in scanning. pp. 1-15, in *Scintillation Scanning in Clinical Medicine*, et. by QUINN, J. L., III, W. B. SAUNDERS, 1964.
14. HARRIS, C. C. BELL, P. R., FRANCIS, J. E., JR., SATTERFIELD, M.D., JORDAN, J. C. & MURRAY, J. P., JR.: Collimators for radioisotope scanning. Chapter 2, pp. 25-65, *Progress in Medical Radioisotope Scanning*, ed. by KNISELEY, R. M., ANDREWS, G. A. AND HARRIS, C. C. Oak Ridge Institute of Nuclear Studies Symposium, TID 7673 USAEC.
15. HARRIS, C. C., JORDAN, J. C., SATTERFIELD, M. M., GOODRICH, J. K., STONE, H. L. & HILL, R.: A collimator for scanning with low-energy photons. *J. Nuc. Med.* 5:653-656, 1964.
16. HEATH, R. L.: Scintillation spectrometry: Gamma-ray spectrum catalogue. IDO-16880-1 AEC Research & Development Report. Physics TID-4500, August, 1964, 2nd edition, Vol. I, p. 14, X-ray Production in Shield.
17. HERRING, C. E.: A universal photorecording system for radioisotope area scanners. *J. Nuc. Med.* 1:83-101, 1960.
18. JOHNS, H. E. & CEDERLUND, J. F.: Basic principles of scintillation counting. pp. 41-57 in *Medical Radioisotope Scanning*. Proceedings of IAEA & WHO, Vienna, February, 1959, published by the International Atomic Energy Agency, Kaertnerring 11, Vienna.
19. JORDAN J. C. & MURRAY, J. P., JR.: Collimators for radioisotope scanning. Chapter 2, pp. 25-65, *Progress in Medical Radioisotope Scanning*, ed. by KNISELEY, R. M., ANDREWS, G. A. AND HARRIS, C. C. Oak Ridge Institute of Nuclear Studies Symposium, TID 7673 USAEC.
- 20a. KUHL, D. E.: Influence of collimator design, photon energy and radiation dose on detection effectiveness in liver scanning. *Phys. in Med. & Biol.* 10:93-105, 1965.
- 20b. KUHL, D. E., CHAMBERLAIN, R. H., HALE, J. & GORSON, R. O.: A high contrast photographic recorder for scintillation counter scanning. *Radiol.* 66:730-739, 1956.
21. MALLARD, J. R. & MYERS, M. J.: The performance of a gamma camera for the visualization of radioactive isotopes in vivo. *Phys. Med. Biol.* 8:165-182, 1963.
22. MATTHEWS, C.M.E.: Comparison of coincidence counting and focusing collimators with various isotopes in brain tumor detection. *Brit. J. Radiol.* 37:531-543, 1964.
23. MCAFEE, J. G., STERN, H. S., FUEGER, G. F., BAGGISH, M. S. HOLZMAN, G. B. & ZOLLE, I.: Tc-99m labelled serum albumin for scintillation scanning of the placenta. *J. Nuc. Med.* 5:936-946, 1964.
24. MCAFEE, J. G., FUEGER, J. G., FUEGER, G. F., STERN, H. S., WAGNER, H. N., JR. & MIGITA, T.: Tc-99m pertechnetate for brain scanning. *J. Nuc. Med.* 5:811-827, 1964.
25. MILLER, W. F., REYNOLDS, J. & SNOW, W. J.: Efficiencies and photofractions for sodium-iodide crystals. *Rev. Scientific Inst.* 28:717-719, 1957.
26. MORGAN, R. H.: *The frequency response functions*. *Am. J. Roentgenol.* 88:175, 1962,

27. MYERS, J. M. AND MALLARD, J. R.: Some long-focusing "depth-independent" collimators for in-vivo radioisotope scanning. *Int. J. Appl. Rad. & Isotopes* 15:725-739, 1964.
28. MYHILL, J.: Theory of multichannel collimated scintillation detectors. *Int. J. Appl. Rad. & Isotopes* 12:10-19, 1961.
29. NEWELL, R. R. SAUNDERS, W. AND MILLER, E.: Multichannel Collimators for gamma ray scanning with scintillation counters, *Nucleonics*, 10 (7):36-40, 1952.
30. ROSSMANN, K.: Measurement of the modulation transfer function of radiographic systems containing fluorescent screens. *Phys. in Med. & Biol.* 9:551, 1964.
31. ROTENBERG, A. D. AND JOHNS, H. E.: Collimator efficiency and design I. Collimator efficiency. *Phys. In Med. & Biol.* 10:51-65, 1965.
32. SHY, G. M., BRADLEY, R. B. & MATTHEWS, W. B., JR.: External collimator detection of intracranial neoplasia with unstable nuclides. E & S LIVINGSTONE, Ltd., 1958, Edinburgh & London.
33. TER-POCOSSIAN, M. M. & EICHLING, J. O.: Autofluorography with an X-ray image amplifier. Medical Radioisotope Scanning, Vol. I. Symp. Proc. IAEA, p. 411, Vienna, 1964.
34. WAGNER, H. N., JR., SABISTON, D. C., JR., MCAFEE, J. G., TOW, D. & STERN, H. S.: Diagnosis of massive pulmonary embolism in man by radioisotope scanning. *New Eng. J. Med.* 271:377-384, 1964.

EMORY UNIVERSITY ANNOUNCES WORKSHOP IN RADIOISOTOPE SCANNING

Emory University School of Medicine will present a second "Workshop in Radioisotope Scanning", October 23-27, 1966, immediately preceding the post graduate course "Radiology of Chest Diseases" to be held October 28-29.

The workshop will consist of daily lectures, seminars, individual conferences, and practical exercises using a variety of scanning instruments and the scintillation camera. The participants will work from a special syllabus prepared for this seminar in order that they may become familiar with the technique and interpretation of scintillation scans. Extensive teaching files will be available for review by the participants.

The course is limited to individuals who have had previous experience with radioisotopes and who wish to add or extend scanning procedures to their diagnostic services.

Guest faculty participating in the workshop include Dr. James Quinn of Chicago; Dr. Douglas Ross and Mr. Craig Harris of Oak Ridge. Registration will be limited.

For further information contact:

Joseph L. Izenstark, M.D.
Division of Nuclear Medicine
Department of Radiology
Emory University School of Medicine
Atlanta, Georgia 30322